

NANO-AMP BEAM CURRENT DIAGNOSTIC FOR LINAC-TO-ESA (LESA) BEAMLINE*

S.T. Littleton†, A.S. Fisher, T. Raubenheimer, SLAC, Stanford, CA, USA
C. Huang, Evergreen Valley High School, San Jose, CA, USA

Abstract

The LESA beamline is designed to transport dark current from the LCLS-II and LCLS-II-HE superconducting linacs to the End Station A for various fixed target experiments. The primary experiment is expected to be the Light Dark Matter eXperiment (LDMX) which required beam currents of a few pA. The operation of the beam line must be parasitic to the LCLS-II / LCLS-II-HE FEL operation. The dark current in the LCLS-II is expected to be at the nA-level which will be below the resolution of most of the LCLS-II diagnostics (it will be degraded before the experiments as necessary). This paper will describe a possible non-destructive diagnostic using synchrotron radiation that could be applied at multiple locations along the LCLS-II and the LESA beamline.

INTRODUCTION

The SLAC Linac to End Station A (LESA) beamline is a staged concept to provide a near-CW beam at 186 MHz and sub-harmonics thereof to the SLAC End Station A (ESA) for experiments in particle physics requiring pA to 25 nA electron beams with multi-GeV electron energy [1]. This capability is achieved parasitically by extracting unused bunches from the LCLS-II/LCLS-II-HE superconducting RF (SRF) linac [2, 3].

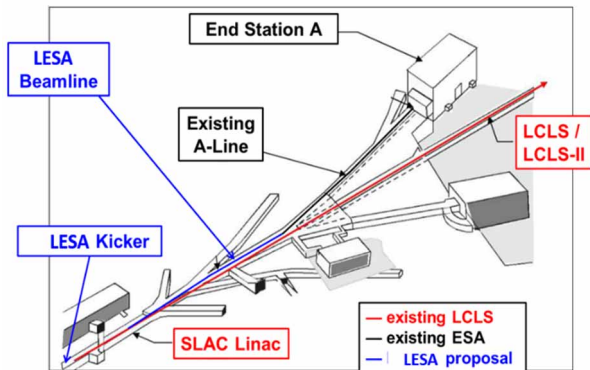


Figure 1: Schematic of LESA beamline starting in SLAC linac and connecting to the A-line.

The LESA beamline begins in Sector 28 of the SLAC linac and continues into the Beam Switchyard, where it connects with the A-line as illustrated in Fig. 1. The beamline consists of (1) a long-pulse kicker and septum magnet to divert low-current bunches off the LCLS-II dump line, (2) a 250m long transfer line from the kicker in Sector 29 to the existing A-line, delivering beam to End Station A, (3) minor improvements in the existing End Station A

* Work supported in part by DOE contract DE-AC02-76-SF00515.

† seantl@stanford.edu.

infrastructure, and (4) an optional laser oscillator that augments the dark current with a well-defined, low-current beam at 46 MHz repetition rate within a ~500 ns macro-pulse between LCLS-II/LCLS-II-HE primary bunches as illustrated in Fig. 2.

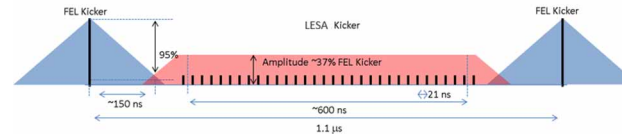


Figure 2: LCLS-II pulse structure showing primary pulses with 10^8 e⁻ and LESA bunches from the gun with 30 e⁻ per bunch. The LESA beam will control the bunch population with an additional seed laser and/or a spoiler/collimation system to deliver final current in the pA to μ A range.

Table 1: LESA Electron Beam Parameters for an Ultra-Low-Current Beam (Baseline) and a Possible Upgrade

Experiment Parameters	Ultra-low-current	Low-current (upgrade)
Energy	4.0 GeV (upgrade to 8.0 GeV in 2027)	4.0 GeV (upgrade to 8.0 GeV in 2027)
Bunch spacing	5.4 – 65 ns	5.4 ns
Bunch charge	0.04 – 10,000 e ⁻	70,000 e ⁻ (10 fC)
Macro pulse beam current	0.1 – 25 nA	2 μ A
Duty cycle	55% (600 ns out of 1.1 μ s)	55% (600 ns out of 1.1 μ s)
Norm. emittance (rms)	~100 μ m; <1000 μ m	~1 μ m
Bunch energy spread	<1%	<1%
IP spot size w/ rastering	4 cm x 4 cm	<250 μ m including jitter
Electrons per year	10 ¹⁵ e ⁻ / year	10 ¹⁹ e ⁻ / year

LESA is being constructed in two stages: the first stage, S30XL, is nearly complete and will demonstrate the dark current extraction from the SRF linac while the 2nd stage, on which construction is just starting, will transport the extracted current to ESA. S30XL will be commissioned in late 2023 while the full LESA beamline is planned to be complete at the end of 2024.

The presently envisioned program for LESA comprises dark sector physics, electron-nuclear scattering measurements for the neutrino program, and a test beam program [4]. Beam parameters are listed in Table 1.

One of the many challenges for the LESA beamline is to quantify the very low current beam in a parasitic manner. The expectation is that the incoming dark current will be at the level of a few nA; if necessary, this will be attenuated before the End Station using a spoiler in the A-line. Ongoing measurements at LCLS-II indicate this level of dark current at the end of the SRF linac [5].

S30XL SYNCHROTRON RADIATION

This paper will address one possible concept for a non-destructive diagnostic using synchrotron radiation and a sensitive x-ray detector that could be applied at multiple locations along the LCLS-II and the LESA/S30XL beamline. The goal is to routinely measure 100 nA to 10 pA beams at the beginning of the LESA/S30XL beamline non-destructively so that we can tune the SRF linac and set the scattering foil correctly.

The LESA/S30XL beamline is illustrated schematically in Fig. 3. As shown, the S30XL kicker and septum extract dark current from the SRF Dump beamline and transport it across the CuRF linac before it is deflected to be parallel to the other beamlines and put into a low-power dump. LESA will transport this into the A-line and ESA.

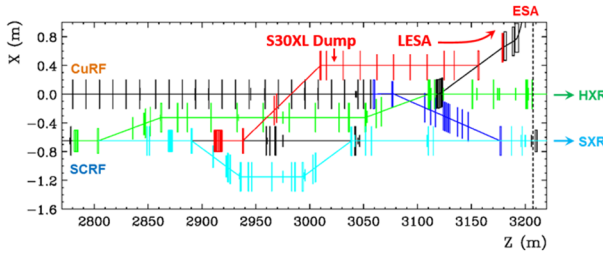


Figure 3: Schematic of the LESA/S30XL beamline (red) along with the SCRF beamline to the HXR FEL (green) and the SCRF beamline to the SXR FEL (blue).

The last dipole in the S30XL line before the Dump is a 1-meter bend and will deflect the beam by 19.1 mrad. The magnetic field is 2.5486 kG at 4 GeV and twice that at 8 GeV. The instantaneous radiated power and the photon critical wavelength are given by the equations:

$$P_\gamma = \frac{cC_\gamma E^4}{2\pi \rho^2} \quad E_c[\text{keV}] = 2.22 \frac{E^3[\text{GeV}]}{\rho[\text{m}]},$$

where E is the electron energy, ρ is the bending radius, and $C_\gamma = 8.85e-5$ [m/GeV³]. With a beamline of 4 GeV and a bending radius of 52.4 meters, the instantaneous radiated power is 3.94×10^8 keV/s. The critical photon energy is 2.71 keV at 4 GeV and 21.68 keV at 8 GeV and the number of photons emitted per second for a photon of energy u can be determined using the equation [6]:

$$n(u) = \frac{P_\gamma}{u_c^2} F\left(\frac{u}{u_c}\right),$$

where u_c is the photon critical energy, E_c , and $F(u/u_c)$ is a function that can be written as:

$$F(\xi) = \frac{9\sqrt{3}}{8\pi} \int_\xi^\infty K_{5/3}(\xi') d\xi',$$

where K is a modified Bessel function. These photons will be swept in angle as the electron traverses the dipole and will have a vertical angle that scales as $1/\gamma$ but depends on the photon energy.

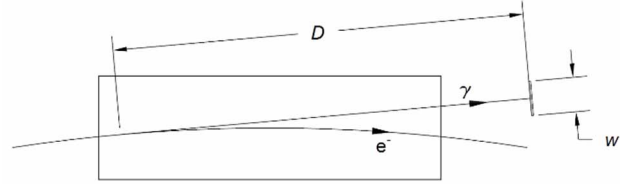


Figure 4: In the diagnostic under consideration, bending magnet radiation is intercepted by a sensitive detector.

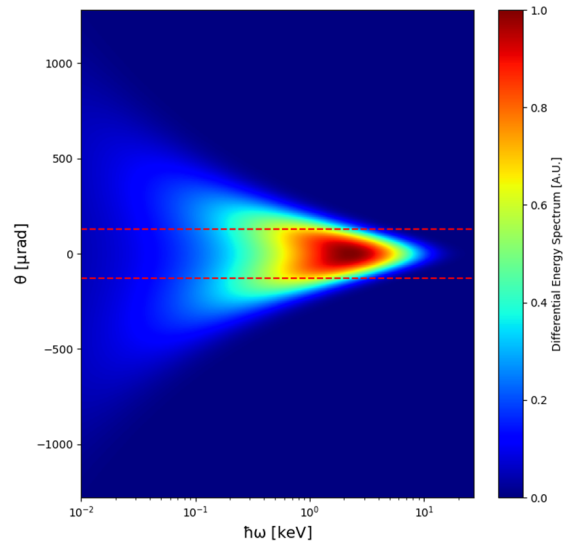


Figure 5: Differential spectrum of the radiation emitted by 4 GeV electrons passing through the bend.

INTERCEPTED SPECTRUM

The spectrum intercepted by a detector of height h and width w a distance D from the location where the radiation is emitted, as shown in Fig. 4, will differ from the full spectrum emitted by the electrons, since some low-energy photons will be radiated at vertical angles greater than $\theta_{max} = h/2D$. To find the intercepted spectrum, we must begin with the full differential spectrum [7], shown in Fig. 5.

$$\frac{d^2I}{d\omega d\Omega} = \frac{e^2}{12\pi\epsilon_0 c} \left(\frac{\omega\rho}{c}\right)^2 \left(\frac{1}{\gamma^2} + \theta^2\right)^2 G(\zeta),$$

where

$$G(\zeta) = K_{2/3}^2(\zeta) + \frac{\theta^2}{1/\gamma^2 + \theta^2} K_{1/3}^2(\zeta)$$

and

$$\zeta = \frac{\omega\rho}{c} \left(\frac{1}{\gamma^2} + \theta^2\right)^{3/2}.$$

Integrating over vertical angles θ between $-h/2D$ and $h/2D$, we find that the spectrum intercepted by a 4.5 mm x 4.5 mm detector at various distances is modified as shown in Fig. 6.

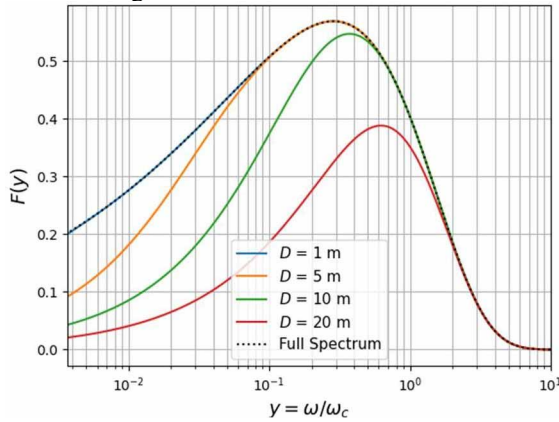


Figure 6: The energy spectrum of the photons intercepted by a 4.5 mm x 4.5 mm detector at various distances from the point where the radiation is emitted.

DETECTOR RESPONSE

We have modeled the response of a 500 μm -thick Cividec B1 CVD diamond detector to the incident synchrotron radiation spectrum, based on data provided by Cividec [8] regarding the mean charge produced in the detector as a function of incident photon energy. Using an eighth-order polynomial fit to the Cividec data, with the constraint that the response goes to zero near the ionization energy of carbon, we multiplied the intercepted photon spectrum by the charge response curve, as shown in Fig. 7. We then integrated over photon energies to estimate the total charge Q produced in the detector per beam electron for detector distances of 1, 2, 5, 10, and 20 m, for both the 4 GeV beam and the 8 GeV LCLS-II-HE beam. The results are shown in Table 2.

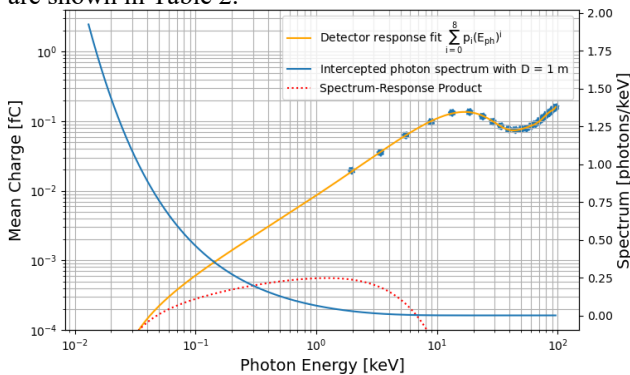


Figure 7: A side-by-side comparison of the photon spectrum and the diamond detector response curve on a log-log plot. The seemingly large region with no response data is a negligible part of the integral.

At 186 MHz, a 10 nA dark current beam would contain roughly 336 electrons per bunch. For $D = 1$ m, the corresponding detector charge would be 1 fC/bunch for the 4 GeV beam or 10 fC/bunch for the 8 GeV beam. When coupled with a Cividec C6 fast charge amplifier [9], with a

gain of 5.4 mV/fC, such a signal may provide useful bunch-by-bunch data, though further amplification may be required locally to prevent noise from contaminating the signal on its way out of the tunnel.

Table 2: Expected Charge Produced by the Cividec Diamond Detector Per Electron in the LESA Beamline

D [m]	Q [fC/e ⁻] (4 GeV beam)	Q [fC/e ⁻] (8 GeV beam)
1	3.1×10^{-3}	3.0×10^{-2}
2	1.5×10^{-3}	1.5×10^{-2}
5	6.1×10^{-4}	6.0×10^{-3}
10	3.0×10^{-4}	3.0×10^{-3}
20	1.3×10^{-4}	1.4×10^{-3}

CONCLUSION

We have investigated the feasibility of using synchrotron radiation emitted by dark current in LCLS-II and LESA to measure the associated nA-level currents. The detector we modeled, a Cividec B1 CVD diamond detector, shows promise as a potential detector for currents at the higher end of the anticipated range of the dark current. To measure lower currents, especially at the pA level, we will explore alternative detectors, such as low-gain avalanche diodes (LGADs) and CCD arrays. The measurement may also be sensitive to the radiation background in the accelerator tunnel. Further studies are needed to characterize the background in the proposed detector location and explore collimation and shielding strategies.

REFERENCES

- [1] T. Markiewicz *et al.*, “The SLAC Linac to ESA (LESA) Beamline for Dark Sector Searches and Test Beams”, *arXiv*. doi:10.48550/arXiv.2205.13215
- [2] T. Raubenheimer, ed., LCLS-II Final Design Report, internal SLAC document, 2015.
- [3] T. Raubenheimer, ed., LCLS-II-HE Conceptual Design Report, LCLSII-HE-1.1- DR-0001 and SLAC-R-1098, Mar. 2018.
- [4] A description of LESA and its science program can be found in SLAC-R-1147. The LESA beamline has been known as DASEL, S30XL, and YABBL.
- [5] Y. Ding, private communication, 2023.
- [6] M. Sands, “The physics of Electron Storage Rings”, SLAC-121, 1971.
- [7] J.D. Jackson, *Classical Electrodynamics*. Wiley. (1998).
- [8] Cividec Instrumentation, “Particle interaction with diamond”, internal working paper for Alan Fisher of SLAC, 2017.
- [9] Cividec Instrumentation, Electronics Application Note.